Polymer 49 (2008) 3582–3589

Contents lists available at ScienceDirect

Polymer

journal homepage: www.elsevier.com/locate/polymer

Structural orientation and tensile behavior in the extrusion-stretched sheets of polypropylene/multi-walled carbon nanotubes' composite

Zaichuan Hou, Ke Wang, Ping Zhao, Qin Zhang, Changyue Yang, Daiqiang Chen, Rongni Du, Qiang Fu*

Department of Polymer Science and Materials, State Key Laboratory of Polymer Materials Engineering, Sichuan University, Chengdu 610065, People's Republic of China

ARTICLE INFO

Article history:
Received 17 March 2008
Received in revised form 25 April 2008
Accepted 3 June 2008
Available online 11 June 2008

Keywords:
Oriented superstructure
Tensile ductility
Nucleating template of nanotubes

ABSTRACT

In this paper, the structural orientation and tensile properties were investigated on the extrusion-elongated sheets of polypropylene (PP)/multi-walled carbon nanotubes' (MWCNTs) composites. The MWCNTs were modified via reactive grafting with octadecylamine to enhance the capability of dispersion in PP matrix. The orientation level of composite sheets was adjusted through adopting various drawn speeds after extrusion, and the structure–property relation was inspected systematically through the combination of two-dimensional wide-angle X-ray scattering, polarized light microscopy and tensile mechanical testing. The tensile behavior of the extrusion-drawn sheet was significantly impacted by both adding MWCNTs and increase of drawn speed. An optimization for simultaneously strengthening and toughening was achieved in the sample with relatively high content MWCNTs prepared upon fast drawn speed. Incorporation of nanotubes didn't alter the orientation degree of crystalline lamellae obviously, but the oriented nanotubes could act as the nucleating templates for the growth of oriented crystalline superstructure. Combined with the present morphological characterizations and the results in other published papers, it was postulated that the oriented superstructure of cylindrulites composed of rigid CNTs as nucleus and PP lamellae as kebabs might be generated in the extrusion-elongated sheets of PP/MWCNTs, which was regarded as the morphological reason for a reinforcing effect on tensile performances.

1. Introduction

Recently, carbon nanotubes (CNTs), including single-walled CNTs (SWCNTs) and multi-walled CNTs (MWCNTs), extensively served as effective reinforcement filler to enhance the mechanical [1–3], thermal [4,5], and electronic [6] properties of polymer materials, due to its unusual characters, such as high mechanical strength/modulus, large ratio surface area, abundant conjugated C–C π bonds and easily generated reactive sites. However, carbon nanotube is strongly affected by Van der Waal's attraction just due to its small diameter and large ratio surface area. These forces give rise to the formation of aggregates, which in turn, make dispersion of CNTs in polymers difficult, resulting in rather poor mechanical and electro-conductive properties. The methods commonly used to incorporate CNTs into thermoplastic polymers can be roughly classified into four strategies: (1) melt compounding of CNTs with polymers [7,8]; (2) solution mixing or film casting of suspensions of CNTs in dissolved polymer [9,10]; (3) in situ polymerization of CNTs–polymer–monomer mixture [11,12] and (4) directly mixing dispersed CNTs with water-dispersible polymer latex in aqueous suspension [13,14].

Among the three strategies for fabrication of polymer/CNTs' nanocomposites, melt compounding seems to be the most convenient, efficient one. At this time, some polymer/CNTs' nanocomposites with excellent properties have been prepared successfully through this approach. Zhang et al. [15] validated that grafted-reaction might occur easily between polystyrene and pristine CNTs' surface upon dynamic melt mixing condition, resulting in CNTs covered by polystyrene shell. Simple melt compounding induced a fine dispersion of CNTs in polyamide 6 and a strong interfacial adhesion between CNTs and polymer matrix was responsible for the remarkable enhancement in mechanical properties [16,17]. In the research by Yang et al. [18], the well dispersion of CNTs and the strong filler/matrix adhesion were achieved via melt compounding of polyethylene (PE) and PE-functionalized CNTs though the matrix was a nonpolar polyolefin, and more importantly, the significant toughening and strengthening could be simultaneously obtained in the as-prepared CNTs-reinforced nanocomposites.

Tensile performance is an important criterion for practical application of polymer products. In order to achieve excellent tensile properties, main attentions were devoted to improve CNTs'

* Corresponding author. Tel.: +86 028 85460953; fax: +86 028 85405402.
E-mail address: qiangfu@scu.edu.cn (Q. Fu).

0032-3861/$ – see front matter © 2008 Elsevier Ltd. All rights reserved.
doi:10.1016/j.polymer.2008.06.008

dispersion and interfacial interaction of CNTs/matrix. A well dispersion of CNTs in polymer is benefit for eliminating stress concentration (defeats of consistent system), while a strong interfacial adhesion is favorable to stress transfer from CNTs to basal polymer. These two issues could be resolved effectively via functionalized modification of CNTs that grafting special groups onto CNTs' surface [19,20]. Unfortunately, in many cases, although the tensile strength, modulus and stiffness were improved significantly, the toughness and flexibility (ductility) were frequently unchanged or obviously decreased [12,21,22]. The key points that predominate the toughness and ductility in nanocomposites should be well understood. Some new mechanisms or knowledge about nanoparticles toughening of polymer matrix during stretching deformation has been proposed in the past literature. In a research concerned carbon nanofiber enhanced ultrahigh molecular weight polyethylene [23], Chen et al. explained the toughening mechanism of prominent improvement in elongation at break as: the tiny nanofibers grafted with alkyl chains played a lubrication role to aid the surrounding polymer chains moving, induced interfacial flow under stretching. Molecular-dynamics studies have suggested that the mobility of the nanoparticles in the polymer might be crucial for introducing new energy-dissipation mechanism that leads to enhanced toughness in the nanocomposites [24]. And Shah et al. [25] presented experimental evidence that nanoparticle orientation and alignment under tensile stress were responsible for this energy-dissipation mechanism, and the mobility of polymer matrix was a precondition for this mechanism to be effective. A logical deduction from the mechanism by Shah et al. was that the pre-orientation of polymer matrix and nanoparticles along tensile deformation direction could remarkably increase the mobility of both, therefore resulting in an improvement in toughness and ductility. This deduction has been approved in our recent study [26], in which excellent ductility was achieved in the oriented injection-molded bars of polypropylene (PP)/MWCNTs' composite.

Another attractive topic about polymer/CNTs' nanocomposite is the anisotropic structure and morphology induced by the incorporation of CNTs with high aspect ratio. Especially, for the practical dynamic processing of semicrystalline polymers concerned shear flow field, when thread-like nanotubes took preferential alignment along shear or stretching direction, they could be regarded as the nucleating templates for the growth of oriented crystallites or typically called 'shish–kebab' superstructure. Such oriented crystalline structures have been found in the stretching of poly(ethylene terephthalate)/CNTs' bars [27], the poly(vinyl alcohol)/CNTs' fibers [28], the drawing HDPE/CNTs' films [29] and the injection-molded bars of poly(butylene terephthalate)/CNTs [30,31] and PP/CNTs' [32] composites. To these oriented semicrystalline polymer/CNTs' systems, oriented crystalline structure and morphology should impact substantially the tensile behavior. However, a distinct demonstration of the relation between structural orientation and tensile properties is by far unavailable or involved seldom in the literature.

In this paper, a succession of our previous research about the toughening mechanism and the structure–property correlation in the oriented PP/MWCNTs' composites [26] was performed on the extrusion-elongated sheets. For tailoring the compatibility between polyolefin matrix and CNTs, a chemically modified method has been developed to successfully produce the nanotubes with branching alkyl chains upon thermally molten reactive conditions [23,33,34]. On the other hand, it has been well proved that the maleic anhydride grafted polyolefin could be used as the compatibilizer for improving dispersion of inorganic nanofillers in polyolefin matrix [35,36]. Interestingly, Yang et al. [18] have found that grafting reaction could take place between maleic anhydride grafted PE and SWCNTs during molten extrusion process, resulted in PE-grafted CNTs. So, in our study, two means were used to ensure a well dispersion of MWCNTs within PP matrix, as that: (1) modification of raw MWCNTs through grafting C18 alkyl chains on the backbones of nanotubes; (2) incorporation of 10 wt% maleic anhydride-grafted PP (PP-*g*-MA) acted as compatibilizer. It should be clarified that a PP/PP-*g*-MA (90/10 wt%) blend was used as the basal polymer (regarded as the pure PP), because (1) the good compatibility between PP and PP-*g*-MA guarantees no obvious phase separation emerges even in the cold solid state; (2) the estimation of the MWCNTs' effect on properties and morphology will be drawn exactly, based on the basal polymer with the same composition. To estimate clearly the effect of structural orientation on the tensile properties, the orientation level of composite sheets was adjusted through adopting various drawn speeds after extrusion, and thus the evolution of tensile behaviors with changed orientation was inspected systematically through combination of two-dimensional wide-angle X-ray scattering, polarized light microscopy and tensile mechanical testing.

2. Experimental

2.1. Materials

A commercially available isotactic polypropylene (trade marked as T30S, Yan Shan Petroleum, China) with $M_w = 39.9 \times 10^4$ g/mol and $M_w/M_n = 4.6$, and a maleic anhydride-grafted PP (PP-*g*-MA) with MA content = 0.9 wt%, $M_w = 21.1 \times 10^4$ g/mol and $M_w/M_n = 3.2$ were used as matrix polymer and compatibilizer, respectively. The raw MWCNTs possess a diameter about 10–20 nm and length about 5–15 μm, and its purity is larger than 95%. Before molten compounding with PP, the pristine MWCNTs were executed grafting reaction with octadecylamine according to the method suggested by Qin et al. [37]. The grafting modification of MWCNTs was elucidated briefly as follows. Pristine MWNTs (50 g) were refluxed 24 h in 800 mL of concentrated nitric acid. The excess concentrated nitric acid was removed by centrifuging. The resulting black solid was washed thoroughly with deionized water until the pH value of the water was about 5–6. The purified MWNTs were dried at 50 °C in a vacuum overnight, and then the purified MWNTs were stirred in 500 mL of fresh distilled thionyl chloride at 70 °C for 24 h to convert the surface-bound carboxylic acid groups into acyl chloride groups. After centrifugation, the remaining solid was washed with anhydrous tetrahydrofuran (THF) and then dried at room temperature under vacuum. A mixture of the resulting solid and 30 g of octadecylamine (ODA) was stirred under N_2 atmosphere at 80 °C for 96 h. After cooling to room temperature, the resulting solid mixture was placed in a Soxhlet extractor. A 300 mL of ethanol was employed as extraction solvent to remove the excess amine. After 24 h, the ethanol solution was discarded, and 300 mL of chloroform was used as extraction solvent to remove the excess amine. After another 24 h, the resulting black solid ($CNT(CONHC_{18}H_{37})_n$) in the Soxhlet extractor was obtained and dried at room temperature under vacuum. And the weight percent of ODA grafted on nanotubes was about 3% calculated from thermal gravimetric analyses (TGA).

2.2. Preparation of PP/MWCNTs' sheets

A series of nanocomposites consisted of PP/PP-*g*-MA/MWCNTs (90/10/*x* wt%; $x = 0$, 0.1, 0.3) were melt-mixed in a TSSJ-2S co-rotating twin-screw extruder. The temperatures were maintained at 160 °C, 175 °C, 190 °C, 200 °C, 200 °C and 195 °C from the hopper to the die and the screw speed was about 120 rpm. Extruded strands of the molten composite were then pelletized. The extruded pellets were secondly extruded into sheets using a Haak single screw extruder (Rheocord System 40) fitted with a slit die of 1.5 mm thickness × 50 mm width. For preparing sheets with different

levels of orientation, several relative drawn speeds were selected as 1, 2, 3, 5 and 7. In the case of 1-folded drawn speed, the rotating rate of the roll is about 0.6 rpm to produce a sheet with a draw ratio (area of extrusion die vs. section area of elongated sheet) of 1. In a convenient manner, the extrusion-elongated sample is thereafter labeled as PPCNT*x*–*y*, where *x* represents the mass percentage content of CNTs multiplied by 10 and *y* is the relative drawn speed. For an instance, PPCNT3–7 indicates a sample with 0.3 wt% MWCNTs prepared upon 7-folded drawn speed.

2.3. Characterizations and mechanical testing

2.3.1. Tensile testing

The tensile experiments were carried out with aid of Shimadzu AG-10TA Universal Testing Machine. The stretching direction of sheets is same as the tensile deformation direction. The moving speed of crosshead was 50 mm/min, and the distance interval for collecting data was 0.25 mm. The measure temperature was about 25 °C. Tensile strength and elongation at break could be directly obtained from the stress–strain curves. The reported values were calculated as averages over five specimens for each composition.

2.3.2. Two-dimensional wide-angle X-ray scattering

The 2D wide-angle X-ray scattering (2D WAXS) experiments were conducted on a SEIFERT (DX-Mo8*0.4s) diffractometer equipped with a 2D Mar345 CCD X-ray detector. The wavelength of the monochromatic X-ray from Mo radiation was 0.71 nm and the sample-to-detector distance was 324 mm. The samples were placed with the orientation (flow direction) perpendicular to the projection beams. The backgrounds of all the 2D WAXS patterns had been extracted thus allowed a qualitative comparison between various samples.

2.3.3. Polarized light microscopy

Morphological observations of PP crystallites' growth were performed on a Leica DMIP polarizing light microscopy (PLM) equipped with a Linkam THMS 600 hot stage under crossed polarizers. The thin slices were cut from the stretching sheets, inserted between two microscopic cover glasses, melted at 180 °C and squeezed to obtain thin films. Then, the slices were held at 180 °C for 2 min to achieve thermal equilibrium. In subsequence, the molten slices were cooled to 120 °C with a rate of −3 °C/min, and then in situ observations of crystallites' growth were implemented during nonisothermal process.

2.3.4. Scanning electron microscopy

To understand the toughening mechanism, a JEOL JSM-5900LV SEM instrument was used to inspect the tensile fractured surface of the as-prepared PP/MWCNTs' composite. The tensile fractured surface was etched chemically by alkyl solvent to expose the MWNTs in PP matrix and then gold-coated and observed under an acceleration voltage of 20 kV.

2.3.5. Differential scanning calorimetry

The thermal analysis of the samples was conducted using a Perkin–Elmer pyris-1 DSC, calibrated by indium. The mass of testing sample was about 5 mg. The sample was first heated to a moderate temperature (180 °C) at a rate of 100 °C/min, holding for 2 min under nitrogen flow; then the melt was cooled down to 140 °C with a cooling rate of −100 °C/min, and isothermal crystallization implemented at 140 °C for 60 min; after isothermal crystallization, the samples were heated to 200 °C and held for 5 min for erasing crystalline structure, then cooled down to room temperature upon a rate of −3 °C/min. In order to obtain the crystallinity in various extrusion-drawn sheets, the samples of as-prepared sheets were directly heated from 20 °C to 220 °C with a rate of 10 °C/min, and then the endothermic enthalpy of melting crystals was gained through integrating area of the melting peak. The calculated endothermic enthalpy vs. the molten enthalpy corresponding to the 100% crystalline PP (taken as 177 J/g [38]), is the crystallinity.

3. Results and discussion

3.1. Tensile behaviors of the stretching sheets

Increasing drawn speed means improvement of extended level of composite sheet, thus induces anisotropic crystalline structure, which can impact the tensile properties substantially. The stress–strain curves, representing the development of tensile behavior with increase of drawn speed, are shown in Fig. 1 for the composite sheets containing different CNTs' loadings. For the pure PP samples of PPCNT0–*y*, as shown in Fig. 1(a), the ductility is inversely proportional to drawn speed. The elongation at break gradually decreases with increasing drawn speed, simultaneously, a moderate increment in tensile strength from 35 MPa for PPCNT0–1 to 44 MPa for PPCNT0–7 is found, indicating a ductile-to-brittle transform in the tensile behavior. As to the samples with 0.1% MWCNTs (Fig. 1(b)), increase of drawn speed also induces enhancement of tensile strength and decrease of ductility. Whereas, compared to the pure PP samples, the decreased amplitude in ductility is somewhat depressed by adding 0.1% MWCNTs. An optimization in both strength and ductility is achieved when increasing the MWCNTs' content to 0.3%, as shown in Fig. 1(c). Unlike to PPCNT0–*y* and PPCNT1–*y*, improvement of extended level of composite sheets does not induce a prominent decrease in elongation at break for the samples of PPCNT3–*y*. Especially for the sample prepared upon the fastest drawn speed, PPCNT3–7 possesses the highest tensile strength and an elongation comparable to that of the sample prepared upon the slow drawn speed. Obviously, incorporation of MWCNTs may influence the development trend of tensile behavior with increase of drawn speed. To demonstrate the effect of adding CNTs on the tensile behavior clearly, some stress–strain curves are picked out from Fig. 1 and plotted as changing CNTs' loading in Fig. 2(a)–(c) for the relative drawn speeds of 1, 5 and 7, respectively. When the drawn speed is slow, adding MWCNTs can enhance the tensile strength, but the elongation at break is somewhat decreased. Improving the relative drawn speed to 5, the ductility is proportional to the loading of CNTs, but the improvement amplitude is limited. For the fastest drawn speed, a significant increase in elongation at break is found when 0.3% MWCNTs was incorporated into PP matrix. While in the following sections the structural orientation and thermal analysis of crystallization will be investigated in detail for the samples of PPCNT*x*–1, PPCNT*x*–5 and PPCNT*x*–7.

3.2. Structural orientation in the stretching sheets

Combination of adding MWCNTs and increase of drawn speed has yielded the optimized tensile property for both strength and ductility. It is expected that the internal structure of composite sheet would be responsible to the excellent tensile performance. Now a question is arising that whether a special crystalline structure has generated in the stretching of PP/MWCNTs' sheets. Thus 2D WAXS measurement was carried out on the stretching sheets. Extrusion-elongated processing has induced well-defined oriented structure in the pure PP or the PP/MWCNTs' composites, as shown in Fig. 3. The effect of MWCNTs' content on structural orientation can be estimated via comparing the left images to the right image. But no obvious changes on the WAXS patterns can be found by altering MWCNTs' content. On the other hand, it can be seen that increasing drawn speed, from the top images to the bottom images, enhances the anisotropic extent of scattering arcs for the crystalline

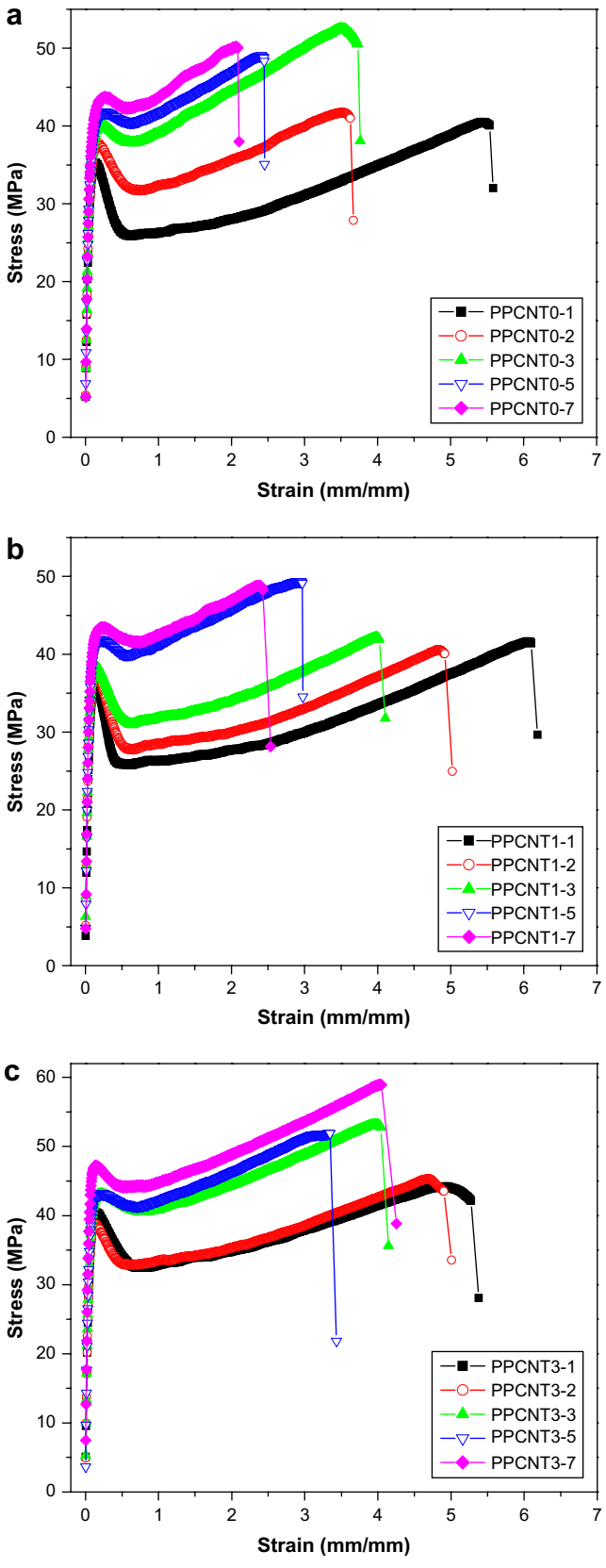

Fig. 1. Stress–strain curves of the PP/MWCNTs' sheets prepared upon different drawn speeds: (a) pure PP, (b) with 0.1% MWCNTs and (c) with 0.3% MWCNTs.

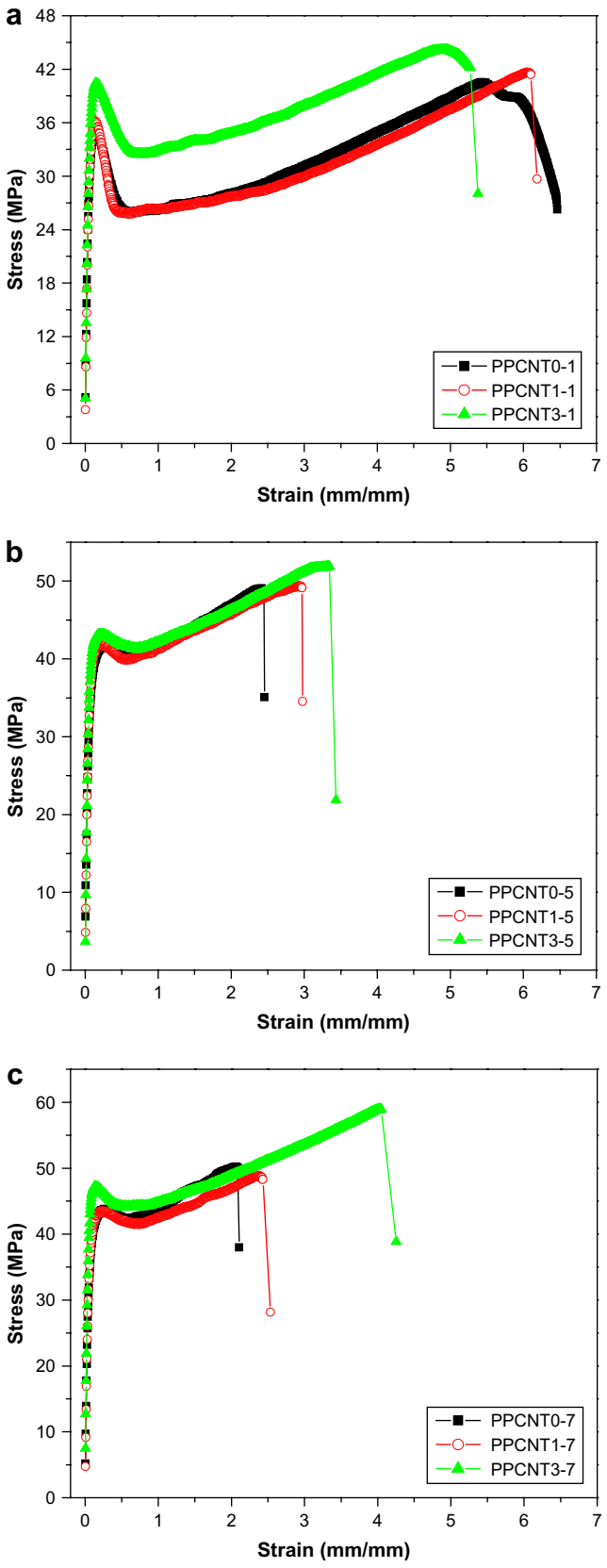

Fig. 2. Stress–strain curves of the PP/MWCNTs' sheets with different loadings of MWCNTs prepared upon: (a) 1-folded, (b) 5-folded and (c) 7-folded drawn speed.

planes of PPα-modification, whatever the sample is with or without MWCNTs. The 5-folded and 7-folded drawn speed has induced remarkably a biaxial orientation of α-crystal in the as-prepared sheets, where both a^*- and c-axis orientations along the shear deformation direction are observed. Pair intensive arcs for (040) plane appear at the equator, indicating preferential orientation of

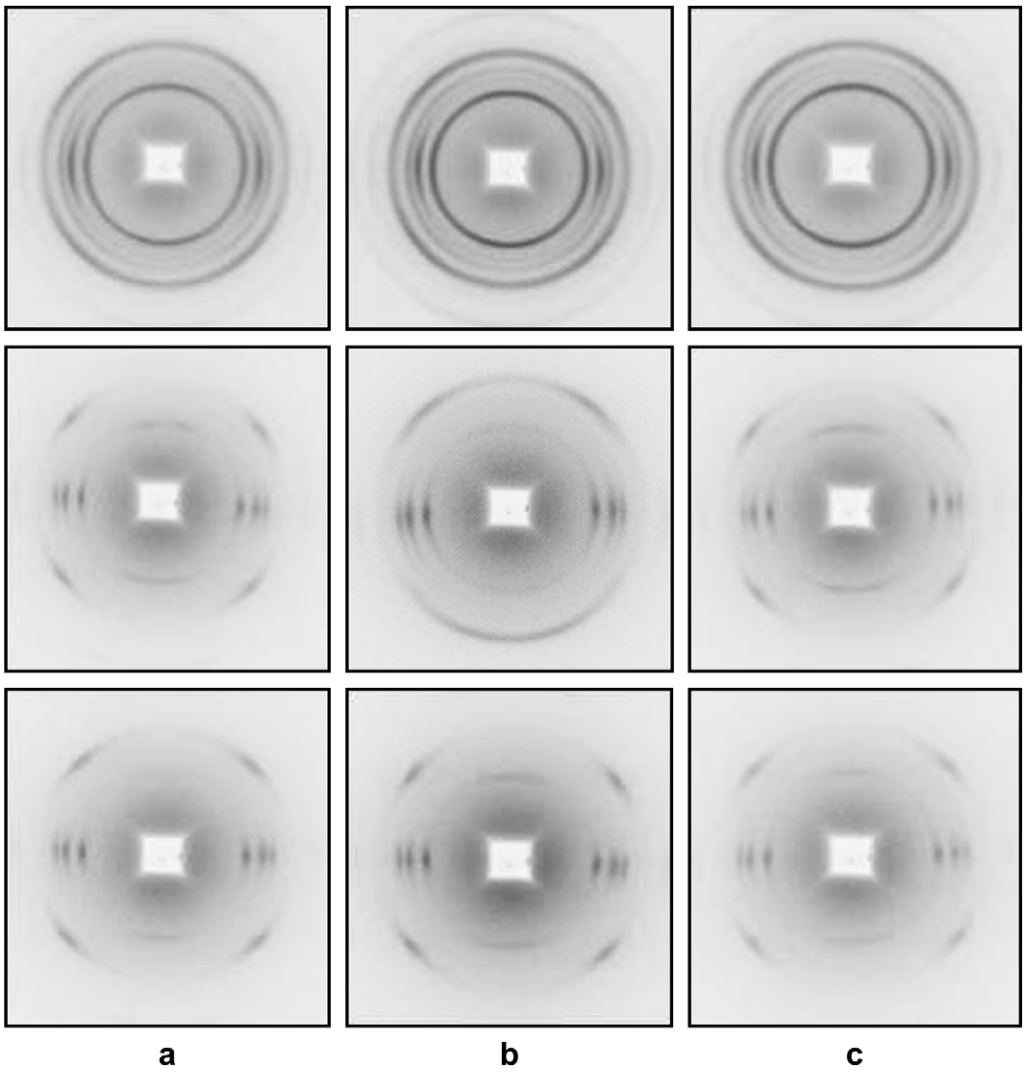

Fig. 3. 2D WAXS patterns of the PP/MWCNTs' sheets with: (a) pure PP, (b) 0.1% MWCNTs and (c) 0.3% MWCNTs. (The stretching deformation direction is vertical and the drawn speed is varied from 1-folded to 5-folded and 7-folded from top to bottom.)

lamellae perpendicular to the stretching deformation direction. In order to estimate the orientation level between different samples quantitatively, Herman's orientation function is used to calculate the orientation degree of (040) plane, which is defined as follows:

$$f_{\mathrm{H}}(\cos\varphi) = \frac{3\langle\cos^2\varphi\rangle - 1}{2}, \tag{1}$$

where $\langle\cos^2\varphi\rangle$ is an orientation factor defined as:

$$\left\langle\cos^2\varphi\right\rangle = \frac{\int_0^{\frac{\pi}{2}} I(\varphi)\cos^2\varphi\sin\varphi\,\mathrm{d}\varphi}{\int_0^{\frac{\pi}{2}} I(\varphi)\sin\varphi\,\mathrm{d}\varphi}, \tag{2}$$

where φ is an angle between the unit within a crystal of interest (e.g., *c*-axis) and a reference direction (stretching deformation direction in this work), and $I(\varphi)$ is the scattering intensity at φ. The calculated orientation functions plotted against relative drawn speed are shown in Fig. 4 for the samples containing 0%, 0.1% and 0.3% MWCNTs. Out our initial expectation, the quantitative estimation of orientation indicates that the effect of adding CNTs on the oriented degree of crystalline structure is inappreciable. For three MWCNTs' contents 0%, 0.1% and 0.3%, the oriented degree of (040) plane is around 0.75, 0.93 and 0.95 for the 1-folded, 5-folded and 7-folded drawn speed, respectively.

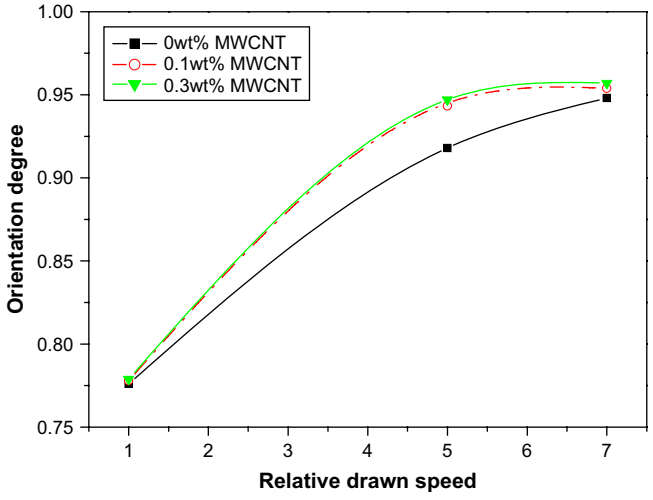

Fig. 4. Evolution of orientation degree with increasing relative drawn speed in various PP/MWCNTs' sheets.

Although the oriented degrees of crystalline structure in the samples with different CNTs' contents are almost identical, the added MWCNTs may significantly impact the modes of nucleation and crystallization of basal polymer. According to the past literature [32,37,39] and our recent study [32], an interesting character of polymer crystallization nucleated by oriented CNTs was that the preferentially aligned CNTs could act as a template for generation of oriented, anisotropic cylindrulites. In this work, the template effect of MWCNTs for anisotropic crystalline superstructure could be also effective for the stretched PP/MWCNTs' composite sheets, which can be evident through re-crystallization observation using PLM. Some nonisothermal re-crystallization processes are shown in Fig. 5. For the pure PP samples (Fig. 5(a) and (b)), only common spherulites are found even extrusion-stretching proceeding under 7-folded drawn speed though a high level of lamellar orientation was detected before melting. Otherwise, incorporation of MWCNTs

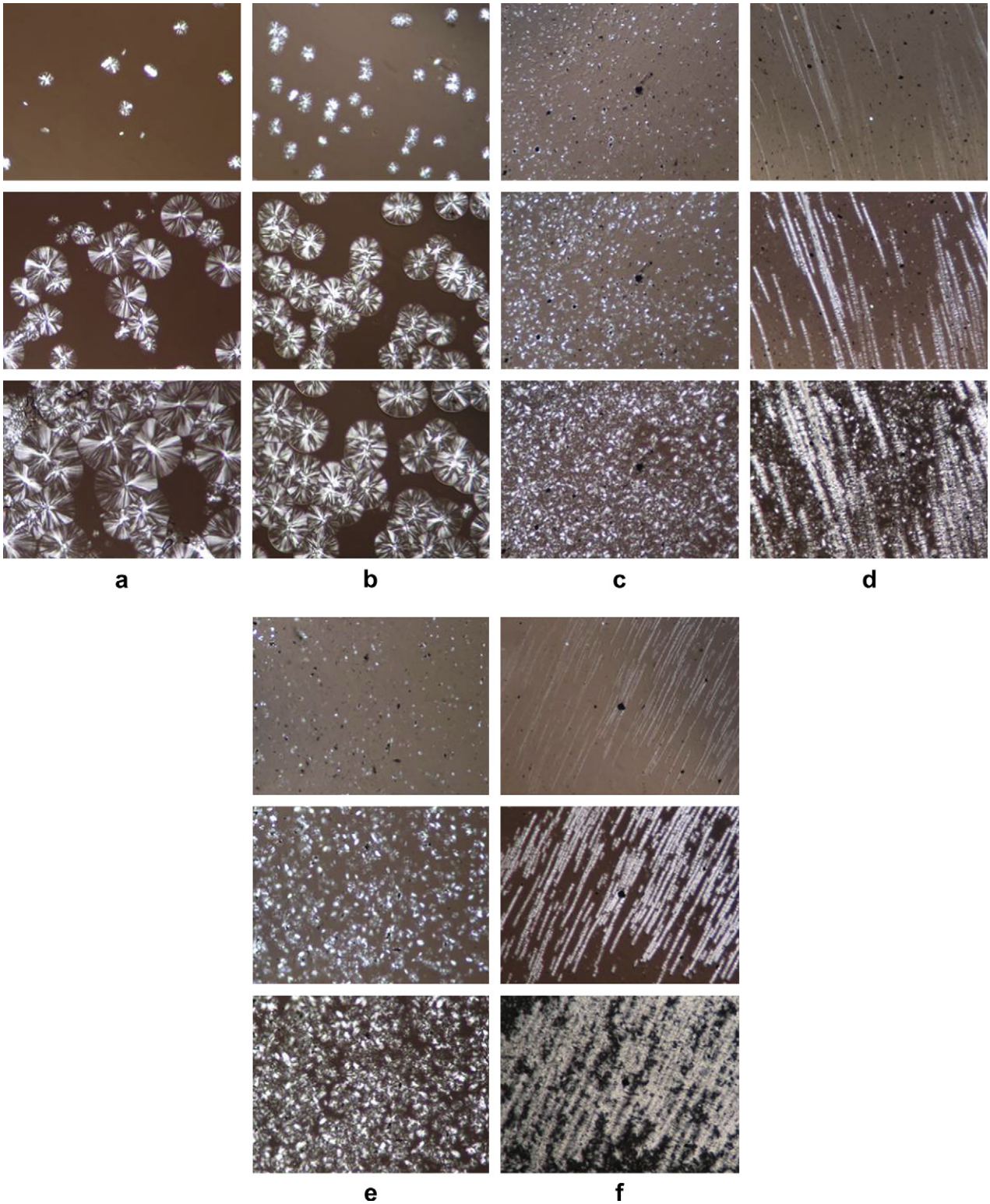

Fig. 5. PLM micrographs of crystalline growth morphologies of re-crystallization for: (a) PPCNT0–1, (b) PPCNT0–7, (c) PPCNT1–1, (d) PPCNT1–7, (e) PPCNT3–1 and (f) PPCNT3–7.

can remarkably alter the crystallization mode, resulted in the oriented, anisotropic cylindrulites when the drawn speed is fast, as shown in Fig. 5(d) and (f) for the CNTs' loading of 0.1% and 0.3%, respectively. Obviously, in these two samples, the oriented nanotubes act as the primary anisotropic nuclei of cylindrulite, namely epitaxy of PP chains occurs on the nanotube surface and the growth direction of lamellae is perpendicular to the surface of oriented CNTs (the stretching deformation direction), resulting in highly oriented crystalline superstructure. Thus it is reasonable to deduce that the oriented crystalline superstructure of cylindrulites nucleated by oriented CNTs could also exist in the composite sheets after extruded-elongation, and is responsible for the observed tensile behavior. Furthermore, an explanation about the term of "cylindrulite" should be defecated as follows. The formation mode of cylindrulites observed in this study is somewhat similar to that of shish–kebab superstructure that: the oriented MWCNTs play the role of shish; the PP lamellae formed on the nanotubes act as kebab. Nevertheless, a precise determination for approving the formation of shish–kebab-like superstructure and the epitaxial crystallization of PP lamellae on MWCNTs are unavailable in the present study, and it may be that the observed anisotropic crystalline superstructures are the later species of shish–kebab subsequent growth, in which radial growth of lamellae has taken place, induced by the second nucleation effect of kebab surface. So we would like to take rather "cylindrulite" than "shish–kebab" to represent the oriented crystalline superstructure observed in the PLM photographs. Another important item for the formation of such oriented cylindrulite is high-level orientation of macromolecular chains, because one can merely find spherulitic structure in Fig. 5(c) and (e) in which the drawn speed is slow, due to a low orientation degree and a fast thermo-relaxation of stretched polymer chains during re-crystallization process. Although the precise structure of MWCNTs/PP co-crystallization was unavailable in our current study, the well-defined "hybrid shish–kebab" crystalline structure, in which the inorganic fibrils acted as shish while polymer lamellae as kebabs, was observed in PE/CNT nanocomposite by Li et al. [40,41] and PE/inorganic whisker nanocomposite by our group [42]. It provides the possibility that the formation of PP/CNTs' co-crystallized structure similar to "hybrid shish–kebab". In this way, an efficient stress transfer is ensured from the nanotubes to the polymer matrix analogous to the case that strong chemical bonding existed at the polymer/nanotube interface [39]; on the other hand, self-reinforcement effect is expected in the oriented crystalline superstructure because rigid nanotubes acted as nuclei to reinforce the whole anisotropic crystal. Consequently, the oriented crystalline superstructure composed of rigid CNTs as nucleus and PP lamellae as kebabs possesses better mechanical performances than the oriented crystalline structure in the pure PP sheet.

3.3. Calorimetric analysis of crystallization

To further investigate the effect of the oriented structure on the re-crystallization of PP, in this section, the crystalline behaviors of extrusion-elongated sheets of composites were inspected using DSC measurements. The thermograms of isothermal crystallization process are shown in Fig. 6(a). For the case that structural orientation could be reserved after the samples were melted at a relative low temperature (180 °C), addition of MWCNTs and increase of drawn speed play a positive influence on the crystallization kinetics of PP, and can facilitate the process of PP crystallization completed within a more shortened time. Obviously, the differences in crystallization kinetics between different samples aren't attributed merely to a melting temperature effect. CNTs acting as nucleating agent and elongated deformation causing stretched conformation of PP chains, these two factors can all result in that crystallization occurred at a higher temperature during the process of preparing

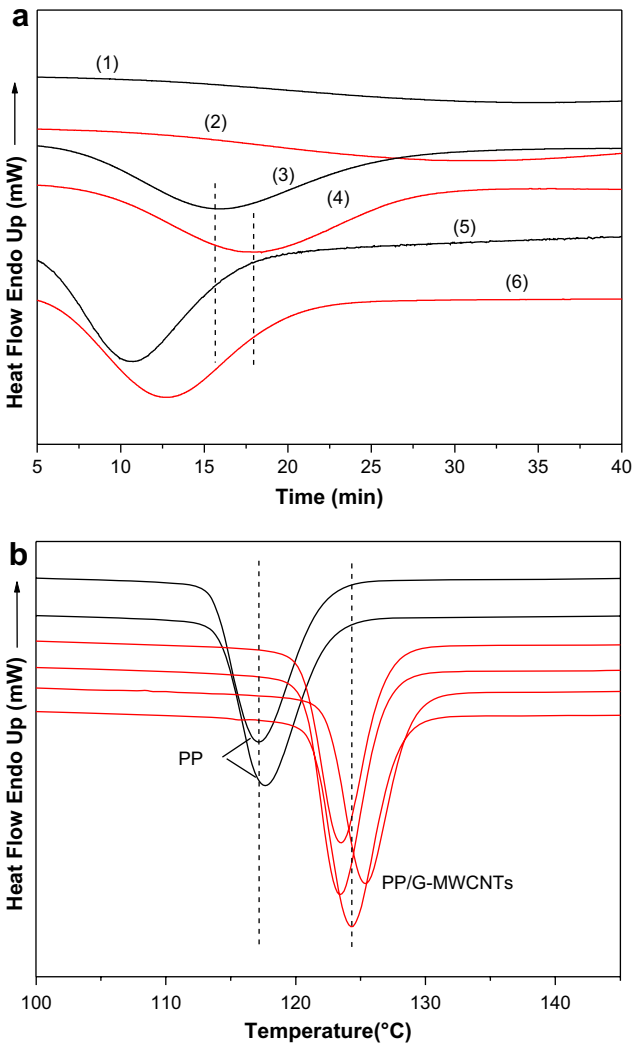

Fig. 6. (a) The curves of isothermal crystallization at 140 °C for 60 min after melting proceeded at 180 °C for 2 min: (1) PPCNT0–1, (2) PPCNT0–7, (3) PPCNT1–1, (4) PPCNT1–7, (5) PPCNT3–1 and (6) PPCNT3–7; (b) nonisothermal crystallization curves after holding at 200 °C for 5 min then cooled down to room temperature upon a rate of −3 °C/min, for the pure PP and the PP/MWCNTs' composites.

the extrusion-elongated sheets, and then generating crystals with thicker lamellae. When melting proceeded under a moderate temperature of 180 °C, the high thermostability of thicker lamellae can ensure more amounts of residual crystallites and preserve high level of oriented conformation of PP chains, which induced faster crystallization kinetics in the subsequent isothermal crystallization performed at 140 °C. Therefore, higher CNTs' loading and faster drawn speed seem to be favorable for a more easy isothermal crystallization. In order to further distinct the roles of nucleation of MWCNTs and elongation-induced orientation on the PP crystallization, nonisothermal crystallization experiments were conducted after erasing thermal history of crystal upon a relative high temperature (200 °C). After melting performed at 200 °C, the positive effect of CNTs' content and drawn speed on the kinetics of nonisothermal crystallization is weak. The corresponding thermograms of nonisothermal crystallization process are shown in Fig. 6(b). For the pure PP samples, the T_c is around at 117 °C whatever the drawn speed is; a increment of 7 °C in the T_c is achieved when adding 0.1% and 0.3% CNTs into PP matrix; while increasing drawn speed does not vary T_c substantially. Deduced from the DSC results, it can be suggested that the structural orientation is not responsible for increasing crystallization kinetics, whereas the

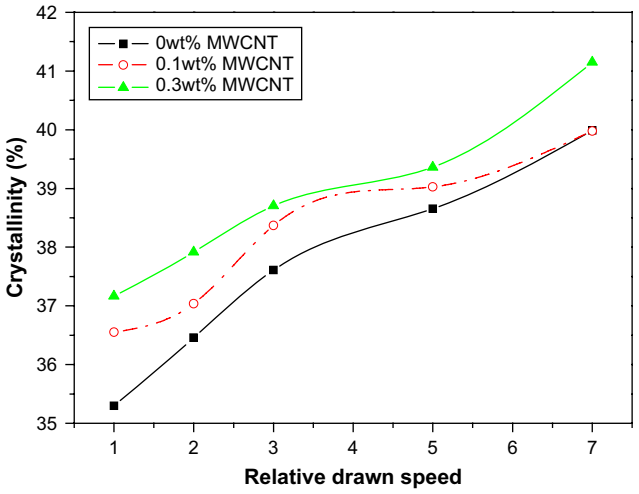

Fig. 7. Evolution of molten crystallinity with increasing relative drawn speed in various PP/MWCNTs' sheets.

nucleating effect of the nanotubes is the dominant issue, no matter what the orientation situation is. Moreover, the roles of incorporation of CNTs and drawn speed (stretching deformation intensity) on the crystalline degrees of various extrusion-drawn sheets are shown in Fig. 7, in which the crystallinity is plotted as a function of drawn speed upon different MWCNTs' contents. Observed from Fig. 7, it can be concluded roughly that the crystallinity is proportional to MWCNTs' contents and drawn speed. Increasing CNTs' content and drawn speed was favorable for generating more amount of crystallites, thus might impact the stiffness and tensile properties of extrusion-drawn sheets more or less. Moreover, one may note that good linear relation of crystallinity vs. drawn speed is found in the pure PP and the composite containing 0.3% MWCNTs whereas the linearity between crystallinity and draw speed is weak in the composite containing 0.1% MWCNTs. The reason is speculated as that: in the pure PP and the 0.3% CNTs' composites, the nucleation mode is uniform that the former is homogeneous nucleation while the later is almost heterogeneous nucleation, thus the crystallization ability is simply dependent on orientation level (drawn ratio); for the relatively low MWCNTs' content, the amount of CNTs is not enough for 100% heterogeneous nucleation, it must be homogeneous nucleation and heterogeneous nucleation coexist, then the modulated effect of orientation on the crystallinity is weak.

4. Conclusion

Highly oriented sheets of PP/MWCNTs' composites were prepared through extrusion-stretched processing. The tensile behavior of the as-prepared sheet was significantly impacted by both of adding MWCNTs and increase of drawn speed. A balance between strength and toughness was achieved in the sample with relatively high content of MWCNTs prepared upon relative fast drawn speed. Incorporation of nanotubes didn't alter the orientation degree of crystalline lamellae, but the oriented nanotubes could act as the nucleating templates for the growth of oriented crystalline superstructure. When combined the present morphological characterizations and the results in other published papers, it was postulated that the oriented crystalline superstructure composed of rigid MWCNTs as nucleus and PP lamellae as kebab is responsible for the enhanced tensile performance in the highly oriented PP/MWCNTs' sheet. In our current study, the MWCNTs' loading is limited to 0.3 wt% and the drawn speed is limited to 7-folded temporarily. However, in the future work, an optimization of simultaneously strengthening and toughening is expected when higher MWCNTs' loading and drawn speed are used.

Acknowledgement

We would like to express our sincere thanks to the National Natural Science Foundation of China for Financial Support (50533050 and 20634050).

References

[1] Sreekumar TV, Liu T, Min BG, Guo H, Kumar S, Hauge RH, et al. Adv Mater 2004;16:58.
[2] Kumar S, Dang TD, Arnold FE, Bhattacharyya AR, Min BG, Zhang XF. Macromolecules 2002;35:9039.
[3] Sen R, Zhao B, Perea D, Itkis ME, Hu H, Love J. Nano Lett 2004;4(3):459.
[4] Geng HZ, Rosen R, Zheng B, Shimoda H, Fleming L, Liu J, et al. Adv Mater 2002;14:1387.
[5] Zou YB, Feng YC, Wang L, Liu XB. Carbon 2004;42:271.
[6] Benoit JM, Corraze B, Lefrant S, Blau WJ, Bernier P, Chauvet O. Synth Met 2001;121:1215.
[7] Jin ZX, Pramoda KP, Goh SH, Xu GQ. Mater Res Bull 2002;37:271.
[8] Andrews R, Jacques D, Minot M, Rantell T. Macromol Mater Eng 2002;287(14):395.
[9] Haggenmuller R, Gonmas HH, Rinzler AG, Fischer JE, Winey KI. Chem Phys Lett 2000;330:219.
[10] Safadi B, Andrews R, Grulke EA. J Appl Polym Sci 2002;84:2660.
[11] Jia ZJ, Wang ZY, Xu CL, Liang J, Wei BA, Wu DH. Mater Sci Eng A 1999;271:395.
[12] Zeng H, Gao C, Wang Y, Watts PCP, Kong H, Cui X, et al. Polymer 2006;47:113.
[13] Grossiord N, Miltner HE, Loos J, Meuldijk J, Mele BV, Koning CE. Chem Mater 2007;19:3787.
[14] Ha MLP, Grady BP, Lolli G, Resasco DE, Ford WT. Macromol Chem Phys 2007;208:446.
[15] Zhang Z, Zhang J, Chen P, Zhang B, He J, Hu GH. Carbon 2006;44:692.
[16] Zhang WD, Shen L, Phang IY, Liu TX. Macromolecules 2004;37:256.
[17] Liu TX, Phang IY, Shen L, Chow SY, Zhang WD. Macromolecules 2004;27:7214.
[18] Yang BX, Pramoda KP, Xu GQ, Goh SH. Adv Funct Mater 2007;17:2062.
[19] Mitchell CA, Bahr JL, Arepalli S, Tour JM, Krishnamoorti R. Macromolecules 2002;35:8825.
[20] Hwang GL, Shieh YT, Hwang KC. Adv Funct Mater 2004;14:487.
[21] Coleman JN, Cadek M, Blake R, Nicolosi V, Ryan KP, Belton C, et al. Adv Funct Mater 2004;14:791.
[22] Moniruzzaman M, Du F, Romero N, Winey KI. Polymer 2006;47:293.
[23] Chen X, Yoon K, Burger C, Sics I, Fang D, Hsiao BS, et al. Macromolecules 2005;38:3883.
[24] Gersappe D. Phys Rev Lett 2002;89:058301.
[25] Shah D, Maiti P, Jiang DD, Batt CA, Giannelis EP. Adv Mater 2005;17:525.
[26] Zhao P, Wang K, Yang H, Zhang Q, Du R, Fu Q. Polymer 2007;48:5688.
[27] Anand KA, Agarwal US, Joseph R. Polymer 2006;47:3976.
[28] Minus ML, Chae HG, Kumar S. Polymer 2006;47:3705.
[29] Zhang QH, Lippits DR, Rastogi S. Macromolecules 2006;39:658.
[30] Garcia-Gutierrez MC, Nogales A, Rueda DR, Domingo C, Garcia-Ramos JV, Broza G, et al. Polymer 2006;47:341.
[31] Garcia-Gutierrez MC, Nogales A, Rueda DR, Domingo C, Garcia-Ramos JV, Broza G, et al. Compos Sci Technol 2007;67:798.
[32] Wang K, Tang C, Zhao P, Yang H, Zhang Q, Du R, et al. Macromol Rapid Commun 2007;28:1257.
[33] Xu D, Wang Z. Polymer 2008;49:330.
[34] Haggenmueller R, Fischer JE, Winey KI. Macromolecules 2006;39:2964.
[35] Perrin F, Ton-That MT, Bureau MN, Denault J. Polymer 2005;46:11624.
[36] Chiu FC, Lai SM, Chen JW, Chu Ph. J Polym Sci Part B Polym Phys 2004;42:4139.
[37] Qin YJ, Liu LQ, Shi JH, Wu W, Zhang J, Guo ZX, et al. Chem Mater 2003;15:3256.
[38] Li JX, Cheung W, Demin L. Polymer 1999;40:1219.
[39] Mylvaganam K, Zhang LC. J Phys Chem B 2004;108:5217.
[40] Li L, Li CY, Ni C. J Am Chem Soc 2006;128:1692.
[41] Li CY, Li L, Cai W, Kodjie SL, Tenneti KK. Adv Mater 2005;17:1198.
[42] Ning N, Luo F, Pan B, Zhang Q, Wang K, Fu Q. Macromolecules 2007;40:8533.